Acc. Chem. Res. **1998,** *31,* 819−826

F_1-ATPase: A Molecular Motor That Hydrolyzes ATP with Sequential Opening and Closing of Catalytic Sites Coupled to Rotation of Its γ Subunit

WILLIAM S. ALLISON

Department of Chemistry & Biochemistry, University of California at San Diego, La Jolla, California 92093-0601

Received March 4, 1998

Elucidation of the crystal structure of the bovine heart mitochondrial F_1-ATPase (MF_1) by Walker and colleagues[1] in 1994 abruptly focused attention on rotational catalysis as the means for coupling ATP synthesis and hydrolysis catalyzed by the F_0F_1-ATP synthase with proton translocation across energy transducing membranes. Rotary catalysis had been postulated earlier by Boyer.[2] However, until the crystal structure of MF_1 became available, it was not possible to design discriminating experiments to test this possibility. Studies subsequently reported by Sabbert et al.[3] with the chloroplast F_1-ATPase and Duncan et al.[4] with the *E. coli* F_1-ATPase were consistent with a rotary mechanism. That rotary catalysis does indeed occur was convincingly demonstated by Noji et al.,[5] who showed that ATP hydrolysis catalyzed by the $\alpha_3\beta_3\gamma$ subcomplex of TF_1-ATPase from the thermophilic *Bacillus* PS3 is coupled to rotation of the γ subunit. Before considering how ATP hydrolysis might be coupled to rotation of the γ subunit, it is pertenent to review the structural characteristics of the ATP synthase.

The F_0F_1-ATP synthases couple proton electrochemical gradients generated by electron transport processes with condensation of ADP with Pi to form ATP in energy transducing membranes as postulated by Mitchell.[6] A model of the F_0F_1-ATP synthase from *E. coli* proposed by Capaldi and colleagues[7] from cryoelectron microscopy and cross-linking studies is shown in Figure 1. F_1 is a globular aggregate perched on two narrow stalks 45 Å above membrane embedded F_0. The F_1 moiety contains the catalytic sites, whereas F_0 mediates transmembrane proton flow.

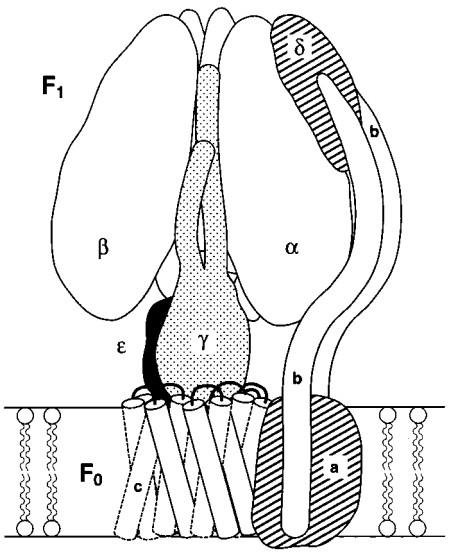

FIGURE 1. A model of the *E. coli* F_0F_1 ATP synthase after Ogilvie et al.[7]

Isolated F_1 is an ATPase comprised of five subunits designated α, β, γ, δ, and ϵ with $\alpha_3\beta_3\gamma\delta\epsilon$ stoichiometry. In *E. coli* F_1, the molecular masses of the α, β, γ, δ, and ϵ subunits are 55.3, 50.3, 31.6, 19.3, and 14.9 kDa, respectively.[8] The α and β subunits are arranged alternately in an $\alpha_3\beta_3$ hexamer. F_1 contains six nucleotide binding sites. Three are catalytic sites located at α/β interfaces, where the majority of bound nucleotides interact with residues on β subunits. Three other nucleotide binding sites, called noncatalytic sites, are located at different α/β interfaces, where the majority of the bound nucleotides interact with residues on α subunits. The F_0 component is an integral membrane protein complex. *E. coli* F_0 is comprised of three gene products designated **a**, **b**, and **c** which are present in $\mathbf{ab}_2\mathbf{c}_{(10-12)}$ stoichiometry and have molecular masses of 30.3, 17.2, and 8.3 kDa, respectively.[9]

The two stalks connecting F_1 to F_0 have different functional roles. One is a rotor, comprised of a γ/ϵ dimer that extends from the aggregate of **c** subunits within the membrane to the $\alpha_3\beta_3$ hexamer of F_1. This serves as a cam shaft that couples rotary motion propelled by proton translocation through F_0 to sequential firing of the three catalytic sites in F_1.[5,10] The second stalk consists of the external domains of the two **b** subunits of F_0 that interact with the δ subunit of F_1, which is bound to the external surface of a single α subunit. This is a stator that holds the $\alpha_3\beta_3$ hexamer in place as the γ subunit rotates within the central cavity.[7]

The **a** and **c** subunits of F_0 are integral membrane proteins which act together in an $\mathbf{ac}_{10-12}$ complex that mediates reversible proton translocation coupled to ATP synthesis and hydrolysis at the catalytic sites of F_1.[9,10] The **c** subunit is a hairpin-shaped protein containing two transmembrane α-helices separated by a short external loop. In at least one **c** subunit, the loop is in contact with the γ and ϵ subunits at the bottom of the rotor stalk.[11] A model has been proposed in which proton translocation

William S. Allison was born in North Adams, MA, in 1935. He earned the A.B. (1957) and M.A. (1959) degrees in chemistry at Dartmouth College and then the Ph.D. in biochemistry with Nathan O. Kaplan at Brandeis University in 1963. After postdoctoral work with J. Ieuan Harris at the Laboratory of Molecular Biology, Cambridge, England, he was Assistant Professor of Biochemistry at Brandeis University from 1966 to 1969. He moved to the University of California at San Diego in 1969 where he is Professor of Chemistry and Biochemistry. His research is primarily focused on the molecular mechanism of the ATP synthase.

10.1021/ar960257v CCC: $15.00
Published on Web 11/04/1998

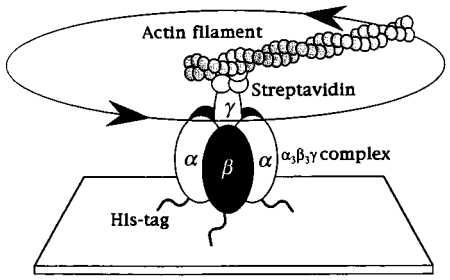

FIGURE 2. Counterclockwise rotation of an actin filament attached to the γ subunit of the TF_1-ATPase driven by ATP hydrolysis demonstrated by Noji et al.[5]

mediated by concerted action of the **a** and **c** subunits during ATP synthesis drives clockwise rotation of a membrane-embedded ring of 12 **c** subunits, which, in turn, drives clockwise rotation of the γ subunit. This model is described in detail in a recent review by Junge et al.[10]

Binding Change Model and Rotational Catalysis

The binding change model proposed by Boyer[2,12] has been the working hypothesis for studies on the molecular mechanism of ATP synthesis catalyzed by F_0F_1 and ATP hydrolysis catalyzed by isolated F_1 for nearly 20 years. The basic tenets of the model in the direction of ATP synthesis are: (1) condensation of ADP with Pi occurs spontaneously without energy input from proton translocation, (2) the three catalytic sites of F_1, which have tight, loose, and open conformations, operate sequentially in binding, interconversion, and release steps, and (3) binding of ADP and Pi to a low-affinity catalytic site promotes simultaneous release of ATP bound to a high-affinity catalytic site that opens at the expense of energy provided by proton translocation.

To accommodate sequential firing of three catalytic sites, it was postulated that proton translocation through F_0 causes minor subunits of F_1 (γ and ϵ) to rotate with respect to the $\alpha_3\beta_3$ hexamer.[2] When the crystal structure of MF_1 was deduced, it became clear that the asymmetric arrangement of the γ subunit with respect to the three heterogeneously liganded catalytic sites is consistent with the postulated rotary mechanism.[1] To test this possibility, Noji et al.[5] remodeled the $\alpha_3\beta_3\gamma$ subcomplex of the TF_1-ATPase. Polyhistidine was introduced at the amino termini of β subunits that allowed attachment of the enzyme to a glass plate coated with Ni^{2+}−nitrilotriacetic acid. A cysteine residue was introduced in the external domain of the γ subunit that provided an attachment site for fluorescently labeled actin filaments of various lengths. The construct is illustrated in Figure 2. When 2 mM ATP plus Mg^{2+} was passed through a flow cell in which the glass plate was mounted, counterclockwise rotation of actin filaments was observed when immobilized subcomplexes were viewed with an epifluorescent microscope. The $\alpha_3\beta_3\gamma$ subcomplex hydrolyzes ATP with a k_{cat} of 52 s^{-1}, predicting a no-load rotational rate of 17 s^{-1}. A rotational rate of 4 s^{-1} was observed when actin filaments of about 1 μm were attached. Clearly, ATP hydrolysis by isolated F_1 is coupled to counterclockwise rotation of the γ subunit when viewed from the bottom of the molecule. This predicts that proton translocation through F_0 drives clockwise rotation of the γ subunit during ATP synthesis.

The remainder of this Account is focused on structure−function relationships in F_1-ATPases, which suggest that rotation of the γ subunit is coupled to opening and closing of catalytic sites during ATP hydrolysis. A model is then proposed for ATP hydrolysis and synthesis that is symmetrical around a common transition state for the reversible process.

Ligation of Catalytic Sites Converts β Subunits from Open to Closed Conformations

In the crystal structure of MF_1 deduced by Abrahams et al.,[1] the elongated α and β subunits are arranged alternately in a hexagonal aggregate. An α-helix, 90 Å long consisting of residues 209−272 at the carboxyl terminus of the γ subunit, extends from top to bottom of the central cavity of the aggregate. The lower part of the carboxyl terminal helix forms an antiparallel coiled coil with an α-helix consisting of residues 1−45 at the amino terminus of the γ subunit. The coiled coil protrudes from the bottom of the aggregate, where it is appended by a short, α-helical spur made up of residues 73−90 of the γ subunit. The remainder of the γ subunit, about 50%, is not sufficiently ordered to diffract to high resolution.

In the crystal structure, the three noncatalytic sites are liganded with MgAMP−PNP. In contrast, the catalytic sites are heterogeneously liganded. One β subunit, designated β_T, is liganded with MgAMP−PNP, and another, designated β_D, is liganded with MgADP. The third β subunit, designated β_E, is free of nucleotides and Mg^{2+}. The α subunits contributing to the catalytic sites of β_T, β_D, and β_E are designated α_T, α_D, and α_E, respectively. Cross-sections of the crystal structure are shown in Figure 3. The α and β subunits, which have about 20% sequence homology, are folded similarly into three domains. A β-barrel is at the top, a nucleotide binding domain composed of alternating α-helices and β-strands is in the middle, and an α-helical domain is at the bottom. Each α and β subunit contributes a top, middle, and bottom loop that points toward the γ subunit. Nearly the entire α and β subunits are sufficiently ordered to be seen in the crystal structure. In contrast, the entire δ and ϵ subunits are not.

Figure 3A shows a cross-section of the $\alpha_3\beta_3\gamma$ complex, revealing the arrangement of the γ subunit with respect to α_E and β_T. The arrangement of γ with respect to α_D and β_E is shown in Figure 3B. The conformations of α_E, α_D, and α_T are nearly identical. In contrast, the conformations of β_T and β_D, which are essentially identical to each other, are vastly different from that of β_E. The liganded β subunits are in closed conformations, whereas β_E is in an open conformation. Figure 3 illustrates that the orientation of helix C (red) with respect to helix B (blue) in the catalytic nucleotide binding domain changes

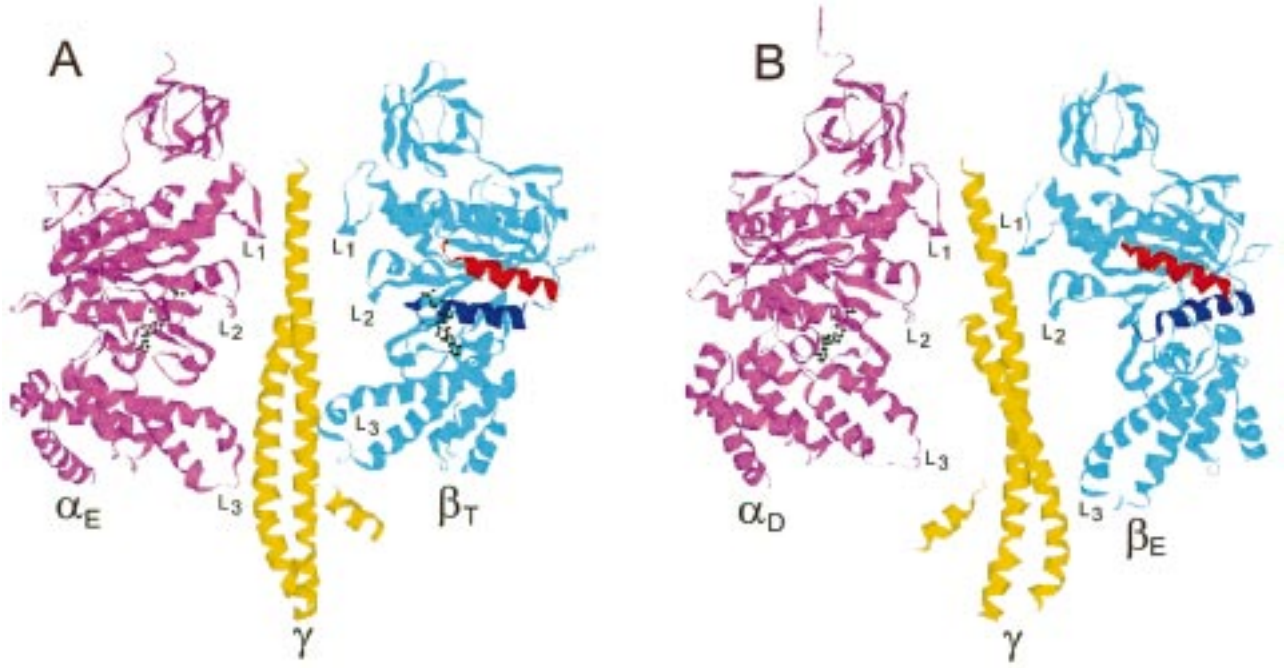

FIGURE 3. Cross-sections of the crystal structure of $MF_1$1: (A) the α_E/β_T cross-section, (B) the α_D/β_E cross-section. L_1, L_2, and L_3 designate the top, middle, and bottom loops in the central cavity emanating from α and β subunits. Helix B is blue and helix C is red in the β subunits illustrated. Figures 2 and 3 were generated with the software program Rasmol provided by R. Sayle (Glaxo Wellcome Research and Development, Greenford, U.K.).

in transition from the open conformation of β_E to the closed conformation found in β_T and β_D. Abrahams et al.[1] indicated that transition from the closed conformation of β_T and β_D to the open conformation of β_E is accompanied by disruption of β-strands and a 30° rotation of the lower portion of the nucleotide binding domain with respect to the α-helical domain at the carboxy terminus.

The crystal structure of MF_1 suggests that catalytic sites convert from open to closed conformations on binding MgATP or MgADP. This premise is consistent with the crystal structure of the $\alpha_3\beta_3$ subcomplex of the TF_1-ATPase elucidated by Shirakihara et al.[13] All three catalytic sites in the $\alpha_3\beta_3$ structure are unliganded and are in open conformations. They are superimposable with β_E of MF_1. In contrast, the conformations of the three α subunits in the $\alpha_3\beta_3$ subcomplex of TF_1, which are also unliganded, are in closed conformations and are superimposable with the liganded α subunits of MF_1.

Functional Side Chains Are Arranged Differently in Liganded and Empty Catalytic Sites

Amino acid side chains which have been implicated by chemical modification and/or mutagenesis studies to have functional roles in catalysis are arranged differently in β_T and β_D opposed to β_E. Rearrangement of critical side chains accompanies reorientation of helix C with respect to helix B in the catalytic nucleotide binding domain illustrated in Figure 3. Functional residues are arranged nearly identically in β_T and β_D, indicating that catalytic sites exist in only two stable conformational states. This view is in contrast to the binding change model that depicts catalytic sites in "tight", "loose", and "open" conformations.[2,12] For the remainder of this discussion, unliganded catalytic sites will be called the T-state and liganded catalytic sites will be called the R-state following the convention adopted for cooperative proteins. In the R-state, the adenine of bound MgAMP−PNP (β_T) and MgADP (β_D) is present in a hydrophobic pocket contributed by the side chains of βTyr^{345}, βPhe^{418}, βVal^{420}, and βPhe^{424}. The relative positions of these residues are nearly the same in β_T and β_D. However, in β_E, the side chain of βTyr^{345} is shifted 3 Å away from the side chain of βPhe^{424} relative to the juxtaposition of these residues in the R-state.

In the R-state illustrated for β_T in Figure 4A, the ϵ-ammonium of βLys^{162} interacts electrostatically with the γ-phosphate of AMP−PNP. The hydroxyl oxygen of βThr^{163} is directly liganded to the Mg^{2+} ion, which is also coordinated with oxygens of the β- and γ-phosphates of bound AMP−PNP. Carboxylate oxygens of βGlu^{192} and βAsp^{256} also interact with Mg^{2+} through water molecules. In β_{TP}, the γ-carboxylate of βGlu^{188} is 4.4 Å from the γ-phosphate of AMP−PNP, where it is hydrogen bonded to a water molecule. From this finding, Abrahams et al.[1] proposed that the carboxylate of βGlu^{188} functions as a general base that activates the water molecule for an in-line attack on the γ-phosphorus during ATP hydrolysis. This is consistent with the dependence of V_{max}/K_m on pH for ATP hydrolysis catalyzed by MF_1, which indicates that the conjugate base of a weak acid with a pK_a of 5.9 is required for catalysis.[14] The enthalpy of ionization of the weak acid is about 1.5 kcal/mol, which corresponds to that of a carboxyl group.[14] Derivatization of βGlu^{188} accompanies inactivation of TF_1 by dicyclohexylcarbodi-

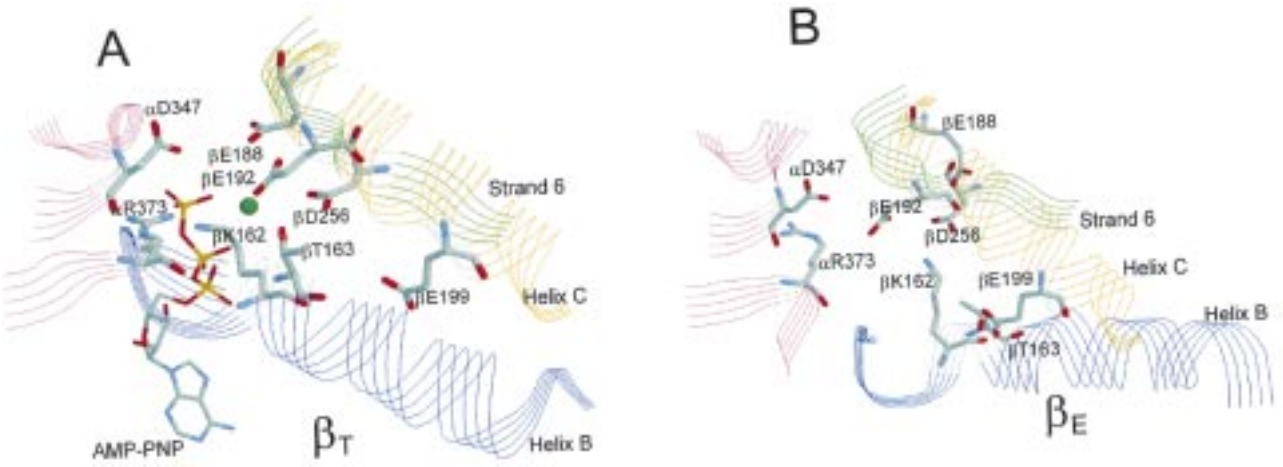

FIGURE 4. Different arrangements of functional amino acid side chains at catalytic sites of MF_1 in the T- and R-states: (A) the R-state of β_T, (B) the T-state of β_E. The Mg^{2+} ion is represented by a green sphere in the illustrations.

imide,[15] whereas βGlu^{199} is derivatized when MF_1 and *E. coli* F_1 are inactivated with dicyclohexylcarbodiimide.[16]

βLys^{162} and βThr^{163} are components of the P-loop, a motif with the consensus sequence G-X-X-X-X-G-K-T/S found at nucleotide binding sites in a variety of proteins.[17] In MF_1, this sequence is ^{156}G-G-A-G-V-G-K-T^{163}. Residues 156−161 form an Ω-loop, whereas βLys^{162} and βThr^{163} are located at the amino terminus of helix B in both the T- and R-states illustrated in Figure 4. In the R → T transition, reorientation of helix C with respect to helix B allows βGlu^{199} to hydrogen bond with βThr^{163} and βLys^{162} to interact electrostatically with βAsp^{256}, which is located in β-strand 6 of the catalytic nucleotide binding domain. In the T-state shown in Figure 4B, the hydroxyl oxygen of βThr^{163} is within 2.9 Å of a carboxyl oxygen of βGlu^{199} and the ϵ-amine nitrogen of βLys^{162} is within 2.7 Å of a carboxyl oxygen of βAsp^{256}. In contrast, in the R-state shown in Figure 4A, these atoms in the respective pairs are 11.3 and 6.7 Å apart.

Chemical modification and mutagenesis studies implicating the ϵ-ammonium of βLys^{162} in catalysis have been thoroughly documented by Weber and Senior.[8] That βThr^{163} interacts with Mg^{2+} was first recognized when it was observed that the βThr^{163}Ser mutant of yeast F_1 has greatly augmented ATPase activity compared to the wild type, little response to activating anions, and substantially decreased sensitivity to inhibition by azide.[18] The activation observed is caused by decreased propensity to entrap inhibitory MgADP in a catalytic site during turnover.[19] This will be discussed subsequently.

Figure 4 also illustrates that the guanidinium of αArg^{373} changes position in the R → T transition. In β_E, it is hydrogen bonded to the carbonyl oxygen of αAsp^{347}, whereas in β_T it interacts electrostatically with the γ-phosphate of AMP−PNP and in β_D it interacts with the β-phosphate of ADP. Abrahams et al.[1] suggested that the guanidinium of αArg^{373} might stabilize a pentacovalent phosphorus transition state during catalysis. This suggestion is consistent with the finding that *E. coli* F_1, in which the corresponding Arg is substituted with Cys, has extremely low ATPase activity.[20]

"Unisite", "Bisite", and "Trisite" ATP Hydrolysis by F_1-ATPases

ATP hydrolysis catalyzed by F_1 and ATP synthesis catalyzed by F_0F_1 have the unusual feature of displaying negative cooperativity of substrate binding and positive cooperativity of catalysis. These phenomena are readily apparent when ATP hydrolyses or ATP syntheses are compared at low vs high substrate concentrations.[21,22] Unisite catalysis, ATP hydrolysis at a single catalytic site, has been characterized by rapidly mixing MF_1 or *E. coli* F_1 with substoichiometric MgATP.[23,24] Under these conditions, association constants for binding MgATP to MF_1 and *E. coli* F_1 are 10^{12} and 4×10^9 M^{-1}, respectively. Both enzymes catalyze net hydrolysis of [γ-^{32}P]ATP at the single catalytic site with a k_{cat} of about 10^{-3} s^{-1}. The rate of hydrolysis of [γ-^{32}P]ATP bound to the single catalytic site accelerates to maximal velocity when excess MgATP is added in a cold chase to saturate empty catalytic sites of much lower affinity. In transition from unisite to multisite ATP hydrolysis, the rate accelerations are 10^6-fold and 10^5-fold for MF_1 and *E. coli* F_1, respectively.

Interpretation of steady-state kinetics of ATP hydrolysis catalyzed by F_1 is complicated by transient entrapment of inhibitory MgADP in a catalytic site when low concentrations of ATP are hydrolyzed. Inhibitory MgADP dissociates from the affected catalytic site as noncatalytic sites are slowly saturated with MgATP.[25] When appropriate measures are taken to minimize or eliminate turnover-dependent entrapment of inhibitory MgADP in a catalytic site, steady-state kinetic analysis reveals two K_m values in the micromolar range. For instance, the $\alpha_3\beta_3\gamma$ subcomplex of TF_1 containing the βThr^{163}Ser substitution does not accumulate inhibitory MgADP during turnover. It displays K_m values of 1.4 and 110 μM with associated k_{cat} values of 14 and 340 s^{-1}, respectively, when assayed with 0.1−2000 μM ATP.[26] Given the rate and binding parameters of unisite catalysis, the two K_m values in the micromolar range with their associated k_{cat} values represent bisite and trisite catalysis, respectively. The k_{cat} for bisite catalysis is about 5% that of trisite catalysis.[21,26]

In the crystal structure of MF_1, the side chain of βTyr^{345} is adjacent to the adenine of MgAMP−PNP and MgADP bound to catalytic sites. After substituting the corresponding residue in *E. coli* F_1 with tryptophan, Weber et al.[27] monitored quenching of fluorescence of the introduced residues to quantify binding of ATP or ADP to catalytic sites with and without Mg^{2+}. In the absence of Mg^{2+}, a single K_d of 71 μM was observed for binding ATP to three catalytic sites. In contrast, in the presence of Mg^{2+}, titration with ATP revealed three K_d values. The first catalytic site filled at the lowest concentration of nucleotide employed and corresponds to the high-affinity site characterized under unisite conditions. The K_{d2} and K_{d3} values for loading the second and third catalytic sites with MgATP are 0.5 and 25 μM, respectively. These values correspond to the K_m values for bisite and trisite catalysis obtained from steady-state analyses of MF_1 and TF_1.

The finding that free ATP binds to catalytic sites noncooperatively, whereas MgATP binds with pronounced negative cooperativity, suggests that catalytic sites do not close unless ATP or ADP are liganded to the Mg^{2+} ion. It is also important to note that physiological concentrations of adenine nucleotides are in the millimolar range. Therefore, unisite and bisite catalysis reflect characteristics of in vitro loading of catalytic sites. The loading process is probably encountered only once in nature when nascent enzyme molecules become assembled.

Role of the γ Subunit in Negative Cooperativity of Substrate Binding

From comparison of binding MgTNP−ATP, a fluorescent derivative of ATP, to the $\alpha_3\beta_3$ and $\alpha_3\beta_3\gamma$ subcomplexes of TF_1 under conditions of unisite catalysis, Kaibara et al.[28] concluded that the γ subunit must be present to demonstrate a single high-affinity catalytic site. However, movement of the γ subunit is not coupled to negative cooperative binding of nucleotides to catalytic sites. Grüber and Capaldi[29] showed that MgATP binds to catalytic sites of *E. coli* F_1 with negative cooperativity when one β subunit is cross-linked to the γ and another to the ϵ subunit.

It is likely that the asymmetric arrangement of the coiled coil of the γ subunit with respect to the 18 loops that line the central cavity of the $\alpha_3\beta_3$ hexamer, illustrated in Figure 3, imparts strain on empty catalytic sites. To account for the high-, medium-, and low-affinity catalytic sites observed under in vitro conditions, it is possible that the induced strain is released in unequal increments as catalytic sites close when they bind MgATP during ATP hydrolysis.

Factors Contributing to Positive Catalytic Site Cooperativity

Both rotation of the γ subunit and transmission of conformational signals from one catalytic site to another that travel through α subunits contribute to positive cooperativity exhibited when F_1-ATPases hydrolyze ATP. The heterogeneous orientation of the γ subunit with respect to the three β subunits in the crystal structure of MF_1 suggests that sequential opening and closing of catalytic sites drives rotation of the γ subunit. The large difference in juxtaposition of the nucleotide binding domain with respect to the carboxyl terminal, α-helical domain in β_E opposed to β_T illustrated in Figure 3 is an integral part of this process. Rotation of the γ subunit is coupled to positive catalytic site cooperativity. García and Capaldi[30] have shown that unisite activity is retained, whereas multisite ATP hydrolysis is abolished when the γ subunit is cross-linked to the β subunit of *E. coli* F_1. It has also been demonstrated that cross-linking the γ subunit to either the α or β subunit of the $\alpha_3\beta_3\gamma$ subcomplex of TF_1 prevents cooperative formation of ADP−fluoroaluminate complexes in two catalytic sites.[31]

Transmission of conformational signals from one catalytic site to another that travel through α subunits also contibutes to positive catalytic site cooperativity exhibited by F_1-ATPases. These conformational signals appear to be independent of rotation of the γ subunit. Inactivation of the $\alpha_3\beta_3$ subcomplex of TF_1 with 7-chloro-4-nitrobenzofurazan is accompanied by derivatization of Tyr311 in a single β subunit, suggesting that cooperative interactions occur during ATP hydrolysis in addition to those that propel rotation of the γ subunit. Altered catalytic characteristics of mutant, bacterial F_1-ATPases show that α subunits participate in positive catalytic cooperativity by transmitting conformational signals from one catalytic site to the next during ATP hydrolysis.[32]

The interface of noncatalytic nucleotide binding sites in α subunits with adjacent β subunits appears to be the site where conformational signals propagated through α subunits during ATP hydrolysis are transferred to β subunits during ATP hydrolysis. In the crystal structure of MF_1, the phenolic hydroxyl of βTyr^{368} is hydrogen bonded with N^3 of AMP−PNP bound to noncatalytic sites at the β_T/α_D and β_D/α_E interfaces, whereas it is 6.8 Å removed from the adenine of AMP−PNP bound at the β_E/α_T interface. Derivatization of βTyr^{368} with 5′-*p*-fluorosulfonylbenzoyladenosine (FSBA) inactivates ATP hydrolysis catalyzed by MF_1, suggesting that this residue plays a role in catalysis.[32] Since βTyr^{368} is distant from catalytic sites, inactivation by FSBA probably reflects interference with positive catalytic site cooperativity required for multisite catalysis.

A Model for ATP Hydrolysis and Synthesis under Saturating Conditions

A model describing the molecular mechanism for ATP hydrolysis by F_1-ATPases must account for sequential participation of catalytic sites coupled to counterclockwise rotation of the γ subunit, transmission of conformational signals from one catalytic site to another through α subunits, and attainment of maximal velocity when three catalytic sites are saturated with MgATP. The step in the catalytic sequence in which transition-state formation and decomposition occurs must also be defined. Considering

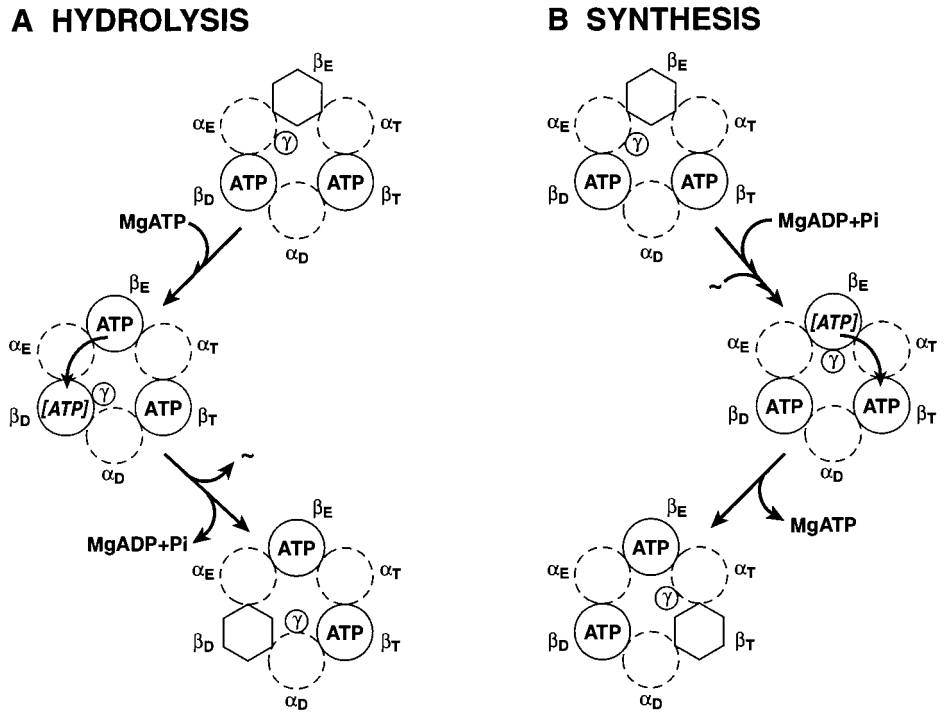

FIGURE 5. Models for the minimal steps of ATP hydrolysis and synthesis under saturating conditions: (A) a round of ATP hydrolysis, (B) a round of ATP synthesis.

that ATP synthesis by membrane bound F_0F_1 is essentially the reverse of ATP hydrolysis catalyzed by F_1, the same minimal criteria apply to ATP synthesis except, in the case of the synthase, clockwise rotation of the γ subunit is driven by proton translocation through F_0.

Figure 5 illustrates models proposed for ATP hydrolysis and synthesis that take these criteria into account. The models were developed with the premise that catalytic sites of F_1 adopt only two stable conformations, rather than three postulated by others.[2,4,8,12] Although rotation occurs in a single step during each round of catalysis, the γ subunit is depicted in the illustrations as rotating in two steps of 60° rather than in a single step of 120° to highlight participation of α subunits in positive cooperativity between catalytic sites. ATP on β subunits represents MgATP bound to catalytic sites. Although noncatalytic sites are saturated with MgATP, the stipled circles representing α subunits are left blank for the sake of clarity. In the models, β_E, β_D, and β_T represent the orientation of β subunits as they appear in the crystal structure of MF_1 rather than different states of ligation of catalytic sites designated in Figures 3 and 4.

Figure 5A depicts dissection of a round of ATP hydrolysis under saturating conditions starting with an empty catalytic site in the T-state and two catalytic sites liganded with ATP in the R-state. The T → R transition accompanying binding of MgATP to β_E promotes counterclockwise rotation of the γ subunit from α_E to β_D and also initiates a conformational signal, indicated by the curved arrow, that is transmitted through α_E to the catalytic site of β_D. Formation of the transition state, designated by ***[ATP]***, is postulated to occur when the rotating γ subunit is in a particular orientation with respect to β_D. The propagated signal promotes the R → T transition of β_D that releases MgADP and Pi as the transition state breaks down to form products. The propagated signal also promotes rotation of the γ subunit from β_D to α_D, thus priming β_T for the next round of catalysis. Consistent with a basic tenet of the binding change model,[2,12] it is thought that concurrent closing of β_E and opening of β_D when MgATP binds to β_E is responsible for the energy yielding step during a round of ATP hydrolysis. This is designated by ~. During ATP hydrolysis by the F_0F_1-ATP synthase, released energy drives proton translocation, whereas ATP hydrolysis by isolated F_1 drives unproductive spinning of the γ subunit.

Figure 5B illustrates dissection of a round of ATP synthesis under saturating conditions. During ATP synthesis, binding of Pi to the *E. coli* F_0F_1-ATP synthase depends on proton translocation through F_0.[8] Therefore, Figure 5B indicates that the T → R transition of β_E occurs with energy-driven, clockwise rotation of the γ subunit from α_E to β_E. This entraps MgADP and Pi in the closed catalytic site where they are condensed to form bound MgATP. The transition state for the condensation is indicated by ***[ATP]***. The energy-dependent T → R transition of β_E initiates a conformational signal, indicated by the arrow, that is transmitted from the β_E/α_T interface through α_T to the α_T/β_T interface, where it promotes release of MgATP from β_T. The R → T transition that releases MgATP from β_T is accompanied by rotation of the γ subunit from β_E to α_T, where it primes β_T, which is now empty, for a round of catalysis.

According to the models, the common transition state for ATP synthesis and hydrolysis designated by ***[ATP]*** forms only when the γ subunit is in a special arrangement with respect to the particular β subunit performing catalysis. Since the γ subunit does not contribute to

catalytic sites, the critcal interaction must be indirect. Modeling of the crystal structure of MF_1 suggests that steric constraints prevent conversion of three β subunits to the closed conformation illustrated in Figure 3 simultaneously.[35] Therefore, to relieve conformational constraint during ATP hydrolysis illustrated in Figure 5A, β_E should be considered partly closed and β_D should be considered partly open when the transition state is formed. For the same reason, during ATP synthesis depicted in Figure 5B, β_E should be considered partly closed and β_T should be considered partly open when the transition state is formed.

The mechanism illustrated in Figure 5B for ATP synthesis, which is based on structural considerations and the observation that maximal velocity is attained when three catalytic sites are saturated with MgATP, conflicts with a basic tenet of the binding change model developed by Boyer.[2,12] The binding change model, which is primarily based on differences in the characteristics of hydrolysis of high vs low concentrations of ATP by F_1, postulates that ATP is synthesized spontaneously at a high-affinity catalytic site and that energy produced by proton translocation through F_0 is required to dissociate ATP from the catalytic site. In contrast, the model illustrated in Figure 5B predicts that energy derived from proton translocation through F_0, which propels rotation of the γ subunit, is used to drive the T → R conversion and concomitant condensation when MgADP and Pi are bound to an open, low-affinity catalytic site. In this process, the proton electrochemical potential is converted to mechanical energy in the form of the torque of the rotating γ subunit, which, in turn, is used to drive formation of a new phosphoanhydride bond.

References

(1) Abrahams, J. P.; Leslie, A. G. W.; Lutter, R.; Walker, J. E. Structure at 2.8 Å of F_1-ATPase from Bovine Heart Mitochondria. *Nature* **1994**, *370*, 621−628.

(2) Boyer, P. D. A Perspective of the Binding Change Mechanism for ATP Synthesis. *FASEB J.* **1989**, *3*, 2164−2178.

(3) Sabbert, D.; Engelbrecht, S.; Junge, W. Intersubunit Rotation in Active F-ATPase. *Nature* **1996**, *381*, 623−626.

(4) Duncan, T. M.; Bulygan, V. V.; Zhou, Y.; Hutcheon, M. L.; Cross, R. L. Rotation of Subunits During Catalysis by *Escherichia coli* F_1-ATPase. *Proc. Natl. Acad. Sci. U.S.A.* **1995**, *92*, 10964−10968.

(5) Noji, H.; Yasuda, R.; Yoshida, M.; & Kinosita, K. Direct Observation of Rotation of F_1-ATPase. *Nature* **1997**, *386*, 299−302.

(6) Mitchell, P. Chemiosmotic Coupling in Oxidative and Photosynthetic Phosphorylation. *Biol. Rev.* **1966**, *41*, 445−502.

(7) Ogilvie, I.; Aggeler, R.; Capaldi, R. A. Cross-linking of the δ Subunit to One of the Three α Subunits Has No Effect on Functioning, as Expected if δ Is Part of the Stator That Links the F_1 and F_0 Parts of the *Escherichia coli* ATP Synthase. *J. Biol. Chem.* **1997**, *272*, 16652−16656.

(8) Weber, J.; Senior, A. E. Catalytic Mechanism of F_1-ATPase. *Biochim. Biophys. Acta.* **1997**, *1319*, 19−58.

(9) Fillingame, R. H. H^+ Transport and Coupling by the F_0 Sector of the ATP Synthase: Insights into the Molecular Mechanism of Function. *J. Bioenerg. Biomembr.* **1992**, *24*, 485−491.

(10) Junge, W.; Lill, H.; Engelbrecht, S. ATP Synthase: An Electrochemical Transducer with Rotatory Mechanics. *Trends Biochem. Sci.* **1997**, *22*, 420−423.

(11) Watts, S. D.; Zhang, Y.; Fillingame, R. H.; Capaldi, R. A. The γ Subunit in the *Escherichia coli* ATP Synthase Complex (ECF_1F_0) Extends through the Stalk and Contacts the c Subunits of the F_0 Part. *FEBS Lett.* **1995**, *368*, 235−238.

(12) Boyer, P. D. The ATP Synthase: A Splendid Molecular Machine. *Annu. Rev. Biochem.* **1997**, *66*, 717−749.

(13) Shirakihara, Y.; Leslie, A. G. W.; Abrahams, J. P.; Walker, J. E., Ueda; T., Sekimoto, Y.; Kambara, M.; Saika, K.; Kagawa, Y.; Yoshida, M. The Crystal Structure of the Nucleotide-free $\alpha_3\beta_3$ Subcomplex of F_1-ATPase from the Thermophilic Bacillus PS3 Is a Symmetric Trimer. *Structure* **1997**, *5*, 825−836.

(14) Godinot, C.; Penin, F. Association of an Amino Acid Residue with a Low p*K* with the Hydrolytic Activity of Mitochondrial F_1-ATPase. *Biochem. Int.* **1981**, *2*, 595−602.

(15) Yoshida, M.; Poser, J. W.; Allison, W. S.; Esch, F. S. Identification of an Essential Glutamic Acid Residue in the β-Subunit of the Adenosine Triphosphatase from the Thermophilic Bacterium PS3. *J. Biol. Chem.* **1981**, *256*, 148−153.

(16) Allison, W. S.; Bullough, D. A.; Andrews, W. W. Identification of Essential Residues in the F_1-ATPases by Chemical Modification. *Methods Enzymol.* **1986**, *126*, 741−761.

(17) Saraste, M., Sibbald, P. R., Wittinghofer, A. The P-loop: A Common Motif in ATP- and GTP-binding in Proteins. *Trends Biochem. Sci.* **1990**, *15*, 430−434.

(18) Mueller, D. M. A Mutation Altering the Kinetic Responses of the Yeast Mitochondrial F_1-ATPase. *J. Biol. Chem.* **1989**, *264*, 16552−15556.

(19) Jault, J-. M.; Dou, C.; Grodsky, N. B.; Matsui, T.; Yoshida, M.; Allison, W. S. The $\alpha_3\beta_3\gamma$ Subcomplex of the F_1-ATPase from the Thermophilic. *Bacillus* PS3 with the $T^{165}S$ Substitution Does Not Entrap Inhibitory MgADP in a Catalytic Site during Turnover. *J. Biol. Chem.* **1996**, *271*, 28818−28824.

(20) Soga, S.; Noumi, T.; Takeyama, M.; Maeda; M. Futai, M. Mutational Replacements of Conserved Amino Acids Residues in the α Subunit Change the Catalytic Properties of *Escherichia coli* F_1-ATPase. *Arch. Biochem. Biophys.* **1989**, *268*, 643−648.

(21) Wong, S.-Y.; Matsuno-Yagi, A.; Hatefi, Y. Kinetics of ATP Hydrolysis by F_1-ATPase and the Effects of Anion Addition, Removal of Tightly Bound Nucleotides, and Partial Inhibition of the ATPase by Covalent Modification. *Biochemistry* **1984**, *23*, 5004−5009.

(22) Hatefi, Y. ATP Synthesis in Mitochondria. *Eur. J. Biochem.* **1993**, *218*, 759−767.

(23) Jault, J-. M.; Allison, W. S. Slow Binding of ATP to Noncatalytic Nucleotide Binding Sites which Accelerates Catalysis Is Responsible for Apparent Negative Cooperativity Exhibited by the Bovine Mitochondrial F_1-ATPase. *J. Biol. Chem.* **1993**, *268*, 1558−1566.

(24) Grubmeyer, C.; Cross, R. L.; Penefsky, H. S. Mechanism of ATP Hydrolysis by Beef Heart Mitochondrial ATPase. *J. Biol. Chem.* **1982**, *257*, 12092−12100.

(25) Al-Shawi, M. K.; Parsonage, D.; Senior, A. E. Kinetic Characterization of the Unisite Catalytic Pathway of Seven β-Subunit Mutant F_1-ATPases from *Escherichia coli*. *J. Biol. Chem*. **1989**, *264*, 15376−15383.
(26) Allison, W. S.; Jault, J-. M.; Grodsky, N. B.; Dou, C. A Model for ATP Hydrolysis by F_1-ATPases Based on Kinetic and Structural Considerations. *Biochem. Soc. Trans.* **1995**, *23*, 752−756.
(27) Weber, J.; Wilke-Mounts, W.; Lee, R. S.-F.; Grell, E.; Senior, A. E. Specific Placement of a Tryptophan Residue in the Catalytic Sites of the *Escherichia coli* F_1-ATPase provides a Direct Probe of Nucleotide Binding: Maximal ATP Hydrolysis Occurs with Three Sites Occupied. *J. Biol. Chem*. **1993**, *268*, 20126−20133.
(28) Kaibara, C.; Matsui, T.; Hisabori, T.; Yoshida, M. Structural Asymmetry of F_1-ATPase Caused by the γ Subunit Generates a High Affinity Nucleotide Binding Site. *J. Biol. Chem*. **1996**, *271*, 2433−2438.
(29) Grüber, G.; Capaldi, R. A. The Trapping of Didderent Conformations of the *Escherichia coli* F_1-ATPase by Disulfide Bond Formation. *J. Biol. Chem*. **1996**, *271*, 32623−32628.
(30) García, J. J.; Capaldi, R. A. Unisite Catalysis without Rotation of the $\gamma-\epsilon$ Domain in *Escherichia coli* F_1-ATPase. *J. Biol. Chem*. **1998**, *273*, 15940−15945.
(31) Dou, C.; Grodsky, N. B.; Matsui, T.; Yoshida, M. Allison, W. S. ADP−Fluoroaluminate Complexes Are Formed Cooperatively in Two Catalytic Sites of Wild-type and Mutant $\alpha_3\beta_3\gamma$ Subcomplexes of the F_1-ATPase from the Thermophilic Bacillus PS3. *Biochemistry* **1997**, *36*, 3719−3727.
(32) Yoshida, M.; Allison, W. S. The ATPase activity of the $\alpha_3\beta_3$ Complex of the F_1-ATPase of the Thermophilic Bacterium PS3 Is Inactivated on Modification of Tyrosine 307 in a Single β subunit by 7-Chloro-4-nitrobenzofurazan. *J. Biol. Chem*. **1990**, *265*, 2483−2487.
(33) Grodsky, N. B.; Dou, C.; Allison, W. S. Mutations in the Nucleotide Binding Domain of α Subunits of the F_1-ATPase from the Thermophilic *Bacillus* PS3 that Affect Cross-talk between Nucleotide Binding Sites. *Biochemistry* **1998**, *37*, 1007−1014.
(34) Esch, F. S.; Allison, W. S. Identification of a Tyrosine Residue at a Nucleotide Binding Site in the β Subunit of the Mitochondrial ATPase with p-Fluorosulfonyl[^{14}C]benzoyl-5′-adenosine. *J. Biol. Chem*. **1978**, *253*, 6100−6106.
(35) Yoshida, M. (personal communication, 1998).

AR960257V